Time-Varying Identification of Ankle Dynamic Joint Stiffness During Movement with Constant Muscle Activation*

Diego L. Guarin[1], *Student Member, IEEE, EMBS*, and Robert E. Kearney[1], *Fellow, IEEE*.

***Abstract*— Dynamic joint stiffness defines the torque generated at the joint in response to position perturbations. Dynamic stiffness is modulated by the angular position and the muscle activation level, making it difficult to estimate during large movements and/or time-varying muscle contractions. This paper presents a new methodology for estimating dynamic joint stiffness during movement and muscle activation. For this, we formulate a novel, nonlinear, dynamic joint stiffness model and present a new algorithm to estimate its parameters. The algorithm assumes that the variability in the model parameters is a function of the mean joint position. Using this methodology we estimated the dynamic joint stiffness at the ankle throughout ramp and hold displacements during a constant muscle contraction. The estimated model accurately predicted the intrinsic and reflex torques produced at the ankle as a response to small position perturbations during large displacement with muscle activation. Preliminary results show that during muscle contraction, ankle intrinsic stiffness estimated during movement is significantly lower than that estimated during quasi-stationary experiments.**

I. INTRODUCTION

Joint impedance, or its inverse *dynamic joint stiffness*, characterizes the mechanical properties of the human joint and defines the relationship between the angular position of a joint and the torque generated around it [1]. A complete understanding of joint stiffness and how it is modulated during functional tasks would have important implications in the study of neuromuscular control [1] and the design of bio-inspired prosthesis [2].

Several approaches have been used to measure dynamic joint stiffness [3]. Our laboratory has focused on using system identification techniques to estimate it as the dynamic relation between the joint angular position and torque [1]. Many of our studies focused on stationary situations, where the operating point (mean joint position and activation level of the muscles about the joint) remain constant through the duration of the trials. This motivation behind this is that the dynamic joint stiffness is heavily modulated by the mean joint position and the muscle contraction level [4]. Therefore, holding these two factors constant significantly simplifies the estimation of the model parameters.

However, most functional tasks involve large, continuous movements and time-varying muscle contractions; we hypothesize that the results obtained during stationary experiments are not valid on this situation and in consequence, new methods that permit the estimation of dynamic joint stiffness during functional tasks are needed.

Some studies have characterized the joint stiffness during non-stationary conditions [5]–[7]. However, they used ensemble methods for parameter estimation, which required hundreds of input-output trials each having the same time-varying behavior. These conditions are difficult to achieve experimentally. In addition, these ensemble methods did not explicitly consider the modulation of joint dynamics stiffness by mean joint position and muscle activation.

This paper introduces a methodology that can be used to estimate dynamic joint stiffness during non-stationary conditions. First, Section II presents a novel time-varying model for dynamic joint stiffness, which not only accounts for the torque generated by small position perturbations, used to excite the system, but for the torque produced by large position changes and time-varying muscle contraction. A novel time-varying identification algorithm for this model is then developed. Section III presents a simulation study demonstrating that the new algorithm accurately estimates the state/time-dependent model parameters. Section IV describes the application or our methodology to some representative experimental data. Section V summarizes and discusses these results.

II. MATERIALS AND METHODS

A. Dynamic Ankle Joint Stiffness Model

When the ankle undergoes a large movement, it's passive properties will generate a torque that varies with the joint angle. If small perturbations are superimposed on the large movements, the response of the ankle will be given by the sum of the intrinsic response from the contractile apparatus, the reflex mediated response, and the response from the passive tissue. In addition, if the muscles about the joint are voluntarily contracted, there will be an additional active component. That is

$$\begin{aligned} T_T(t) =& T_P(\theta_m) + T_A(t) + T_I(\theta_p; T_P, T_A) \\ &+ T_R(\theta_p; T_P, T_A), \end{aligned} \tag{1}$$

where T_T is the total torque at the ankle, T_P is the passive torque produced by changes in the mean ankle position (θ_m), and T_A is the torque produced by active muscle contractions. T_I and T_R are the incremental responses to the small position perturbations (θ_p), produced by the intrinsic and reflex mechanisms response and are modulated by T_P and T_A. During stationary experiments, the passive and active components remain constant through the trial, greatly simplifying (1).

*This work was supported by the Canadian Institutes of Health Research (CIHR), and Le Fonds de recherche du Québec Nature et technologies (FQRNT).

[1]The authors are with the Biomedical Engineering Dept, McGill University. 3775, rue University, room 316 Montral, QC. H3A 2B4 Canada. Email: diego.guarinlopez at mail.mcgill.ca

The incremental torque generated by the small position perturbations can be modeled by two parallel pathways. The first, whose input is joint position, represents intrinsic dynamics and can be modeled by a second order system composed by stiffness (K), viscosity (B) and inertia (I). The second, whose input is joint velocity, represents stretch reflex dynamics and is comprised of a series connection of a delay, a differentiator, a static nonlinearity and a low-pass system [1].

Fig. 1 shows this model with the intrinsic and reflex components appearing as functions of mean joint position and time instead of passive and active torque. The measurement noise is $v(t)$ and a final noisy version of the total torque is $\widetilde{T}_T(t)$.

The only signals available for direct measurement are the mean joint position ($\theta_m(t)$), the small position perturbations ($\theta_p(t)$), and the noisy total torque ($\widetilde{T}_T(t)$). All the other signals must be estimated.

1) Model re-parametrization: The model in Fig. 1 is a complex, state/time-dependent, nonlinear model whose parameters are difficult to estimate. We propose a new model parametrization to simplify the identification. First, the static nonlinearity in the reflex pathway is approximated as

$$\begin{aligned}\bar{\dot{\theta}}_p\left(t-\Delta\right) &= g\left(\dot{\theta}_p\left(t-\Delta\right);\theta_m,t\right)\\ &\approx \sum_{s=0}^{S}\gamma_s\left(\theta_m,t\right)\Gamma_s\left(\dot{\theta}_p\left(t-\Delta\right)\right),\end{aligned} \tag{2}$$

where $g(\bullet;\theta_m,t)$ is the true static nonlinearity, $\Gamma_s(\bullet)$ are pre-defined basis function (e.g Tchebichev polynomials), and $\gamma_s(\theta_m,t)$ are state/time-dependent weights. Second, the state/time-dependent parameters are approximated as

$$K\left(\theta_m,t\right) \approx \sum_{d=0}^{D} k_d\Gamma_d\left(\theta_m\right) + \sum_{j=1}^{J} h_j\Gamma_j\left(t\right), \tag{3}$$

where k_d and h_j are constant weights. Finally, as there is no simple way to estimate the muscles activation, the sum of passive and active torques is approximated by the time/position-dependent series given by

$$T_{PA}\left(\theta_m,t\right) \approx \sum_{q=0}^{Q}\alpha_q\Gamma_m\left(\theta_m\right) + \sum_{p=1}^{P}\beta_p\Gamma_p\left(t\right), \tag{4}$$

where α_q and β_p are constant weights.

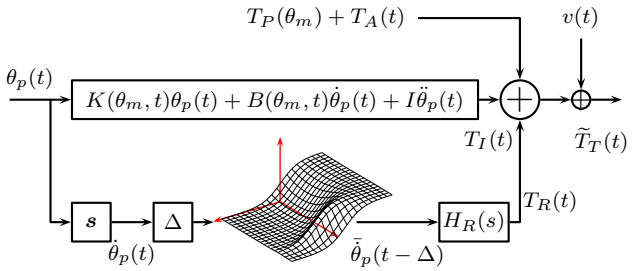

Fig. 1. Ankle dynamic joint stiffness model. The total torque is comprised by the sum of intrinsic, reflex, passive and active components. The model parameters depend on the joint meant position and the time.

B. Parameter Estimation

The identification algorithm is based on that of Kearney *et. at* [1] but exploits the new parametrization. It is an iterative algorithm that estimates the components of each pathway by removing the contributions from the other pathways before applying an identification procedure. It proceeds as follows:

1) Use $\theta_p(t)$ to numerically calculate $\dot{\theta}_p(t)$, $\ddot{\theta}_p(t)$, find Δ from EMG signal, set $\widehat{T}_R^0(t) = \widehat{T}_{PA}^0(t) = 0$, $\%VAF^0 = 0$ and the counter $\lambda = 0$.
2) Estimate the intrinsic torque as
$$\widetilde{T}_I(t) = \widetilde{T}_T(t) - (\widehat{T}_R^\lambda(t) + \widehat{T}_{PA}^\lambda(t)).$$
3) Use $\theta_p(t)$, $\dot{\theta}_p(t)$, $\ddot{\theta}_p(t)$, $\widetilde{T}_I(t)$ and the basis functions to estimate the parameters of the intrinsic pathway using the least squares algorithm. Use these parameter estimates to compute the intrinsic torque $\widehat{T}_I^\lambda(t)$.
4) Estimate the passive and active torque as
$$\widetilde{T}_{PA}(t) = \widetilde{T}_T(t) - (\widehat{T}_I^\lambda(t) + \widehat{T}_R^\lambda(t)).$$
5) Use $\widetilde{T}_{PA}(t)$, $\theta_m(t)$ and the basis functions to estiamte the coefficients of (4) using the least squares algorithm. Use these estimated parameters to compute the passive and active torque $\widehat{T}_{PA}^\lambda(t)$.
6) Estimate the reflex torque as
$$\widetilde{T}_R(t) = \widetilde{T}_T(t) - (\widehat{T}_I^\lambda(t) + \widehat{T}_{PA}^\lambda(t)).$$
7) Use $\dot{\theta}_p(t-\Delta)$ and $\widetilde{T}_R(t)$ to estimate the parameters of the reflex pathway using the algorithm presented in [8]. Use the estimated parameters to compute the reflex torque $\widehat{T}_R^\lambda(t)$.
8) Compute the total torque as
$$\widehat{T}_T^\lambda(t) = \widehat{T}_I^\lambda(t) + \widehat{T}_R^\lambda(t) + \widehat{T}_{PA}^\lambda(t)$$
and calculate the variance accounted for (%VAF) between the measured and predicted torques as
$$\%VAF^\lambda = \left[1 - \frac{\sum\left(\widetilde{T}_T(t) - \widehat{T}_T^\lambda(t)\right)^2}{\sum\left(\widetilde{T}_T(t)\right)^2}\right] \times 100\%$$
9) If there is significant difference between $\%VAF^\lambda$ and $\%VAF^{\lambda-1}$ set $\lambda = \lambda + 1$ and go to 2, else finish.

Some components of this algorithm haven been presented and validated elsewhere [8].

III. Numerical Validation

To validate our algorithm we simulated the model presented in Fig. 1 with a parameter set that provided an output similar to that observed in experiments. The simulation was performed in Matlab for 11s at 1kHz, signals were decimated to 100 Hz for further analysis. Fig. 2A shows the input signal, with the large position changes in red and the small perturbations in blue. Fig. 2B shows the passive (magenta) and the noise-free total (blue) torques. Panels C and D present the simulated intrinsic and reflex torques. For this simulation $T_A(t)$ was set to zero. The additive noise was non-white (low-pass filtered, 6Hz cut-off frequency) and the ratio between the power of the noise and the sum of the intrinsic and reflex components was 10 dB.

Fig. 3 shows with red lines snapshots of the true system dynamics at three times. The first row gives the frequency

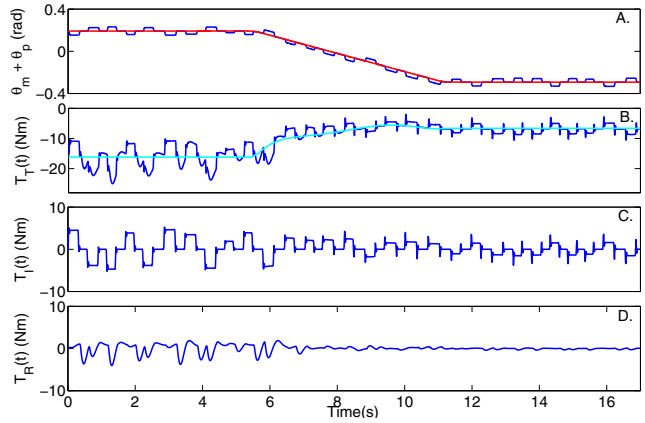

Fig. 2. Typical simulation trial.

response of the intrinsic dynamics at t=1s, t=4s and t=10s. These times correspond to $\theta_m(1) = 0.2$ rad, $\theta_m(4) = 0.0$ rad and $\theta_m(10) = -0.3$ rad so they give a clear idea of how the dynamics changed through the motion. The last two rows present the elements of the reflex pathway; the middle row shows the shape of the static nonlinearity while the last row presents the frequency response of the reflex dynamics which was time-invariant.

A. Numerical Results

One hundred Monte Carlo trials, each with a new noise sequence were simulated. The blue traces in Fig. 3 are the dynamics estimated in each of the simulation trials. It is evident that the intrinsic and reflex components were properly estimated; the results for all other times were equally good. The %VAF between the simulated (noise free) and predicted total torques varied between 99.6% - 99.8%. Furthermore, the %VAF between the simulated and predicted intrinsic and reflex torques varied between 98.8% - 99.9%, and 98.3% - 99.2% respectively.

IV. Experimental Validation

Next, the algorithm was applied to experimental data. The experiment was performed on two healthy male subjects, aged 27 and 30 who provided their informed consent. The

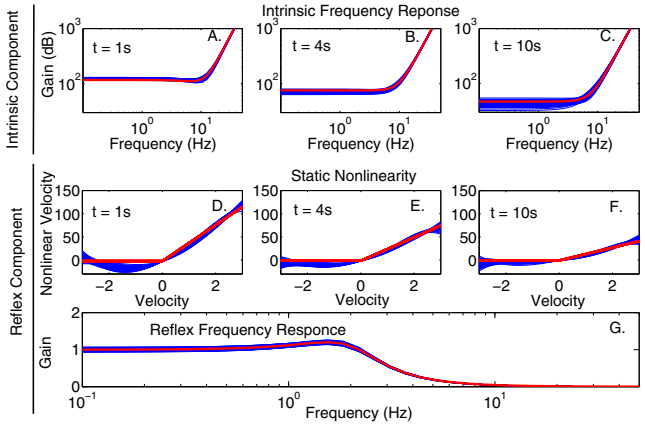

Fig. 3. Simulated (red) and estimated (blue) parameters. First row shows the intrinsis frequency response at certain time instants; last two rows present the reflex static nonlinearity and frequency response.

experimental procedures were approved by the Institutional Review Board. Subjects lay supine with the left foot attached to the pedal of a stiff actuator by means of a custom made fiberglass boot. Ankle position, torque and EMG signal from the ankle muscles were recorded at 1 kHz and then decimated to 100 Hz for further analysis. See [1] for further details.

Two types of movements were studied: quasi-stationary movements, and continuous imposed movements. The objective was to study how the ankle's mechanical properties varied during movement and the effect of muscle activation while avoiding the complexity of time-varying activation.

1) Quasi-Stationary Imposed Movements: The subject's ankle was moved to different discrete positions between 0.2 rad and -0.3 rad (negative position means plantarflexion). During each trial, the mean position was held constant and small perturbations (0.04 rad peak to peak) were applied to the ankle. Each trial lasted for 30s and was performed when subject was relaxed and while the subject contracted its triceps surae (TS) to 10% of the Maximum Voluntary Contraction (MVC). This contraction level was selected because it is expected that the reflex response will be enhanced [4]. To achieve this, the torque produced at MVC and the passive torque at the desired ankle position were measured beforehand. During the trial, the desired position was maintained by the stiff actuator and the subject was asked to contract its TS while a low-pass (0.7 Hz) version of the total minus the passive torques was provided as feedback. In this way, the subject could see only the voluntarily produced torque.

2) Continuous Imposed Movements: The subject's ankle was moved continuously between 0.2 rad and -0.3 rad while small perturbations were applied. The experiment lasted 18s; during the first 6s an initial position was held. Next, the ankle was moved in a ramp with a speed of 5°/s for 6s. Then, the ankle was held at the final position. The experiment was performed during rest and activation of the TS to 10% MVC.

Fig. 4 shows typical trials during rest (left column) and activation (right column). The top panels show the ankle position, comprising by small perturbations ($\theta_p(t)$) superimposed on large position changes ($\theta_m(t)$), the middle panels show the measured torque ($\widehat{T}_T(t)$); a considerable difference in the torque levels between the initial and final positions can be observed. Panels C and F show the rectified EMG from the gastrocnemius (GM) as a representation of the TS activity. The reflex mediated response (spikes) are clearly much larger in the active case than at rest.

A. Experimental Results

The new algorithm was used to estimate the parameters of the model for the quasi-stationary and the continuous movement experiments. In the first case, the elements of the expansions presented in (3) and (4) were limited to the zero order (constant) element while in the second case, the maximum order of the expansion was increased accordingly to capture the variability in the parameters. As the muscles contraction level was almost constant during each trial we did not consider the parameter's time dependency.

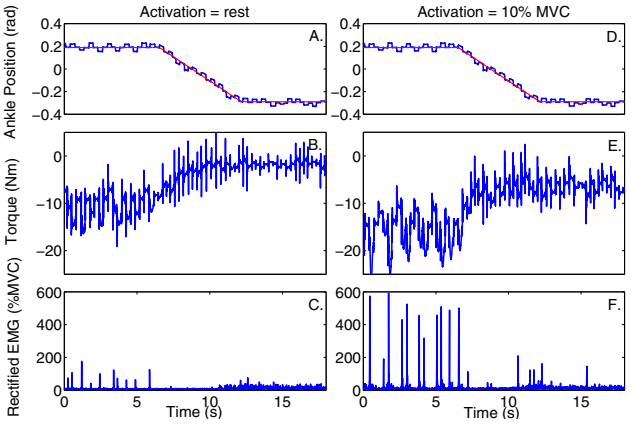

Fig. 4. Data measured during a typical trial during rest (left column) and activation (right column).

Fig. 5 presents the predicted torques for one subject for rest (left column) and activation (right column) during the ramp and hold experiment. The dotted vertical lines in all the panels indicates the beginning of the movement. The top panels shows that the measured (red) and predicted (blue) torques are in good agreement; the %VAF between both torques was close to 96% in all the trials. The magenta lines show the predicted passive and active torque. The middle an bottom panels show the predicted intrinsic and reflex torques as a function of time; there is a significant modulation after the beginning of the movement.

Fig. 6 presents the estimate of $K(\theta_m)$ for the quasi-stationary (red circles) and continuous (blue line) movements, for both subjects during rest and activation. During rest there was no significant difference between the two movement types. In contrast, during activation the intrinsic stiffness was up to 40 % lower during continuous movement than that estimated during the quasi-stationary experiments.

V. DISCUSSION

This documents presents a new model of dynamic ankle stiffness that is able to predict the response not only to small position perturbations, necessary to excite the system, but to large position changes which makes the parameters of the model state-dependent. We also presented a new algorithm

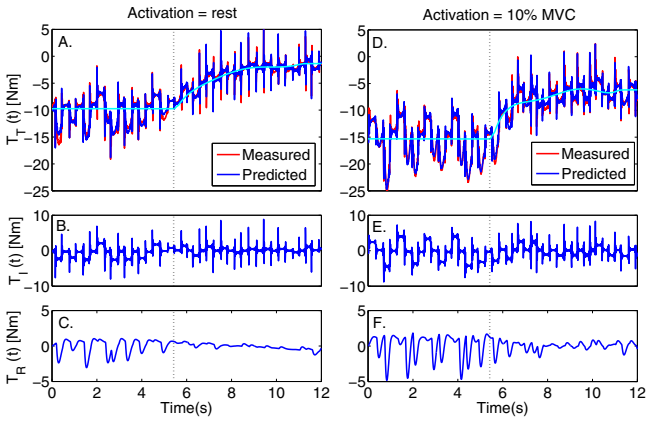

Fig. 5. Example of measured (red) and predicted (blue) torques during rest (left column) and activation (right column).

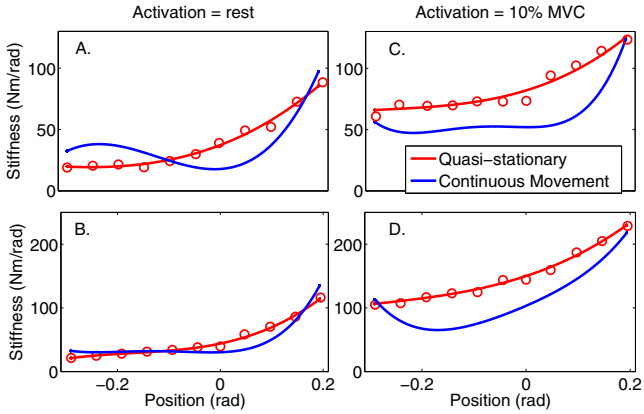

Fig. 6. Ankle intrinsic stiffness ($K(\theta_m)$) estimated during quasi-stationary (red dots) and continuous (blue lines) movement experiments during rest (left column) and activation (right column) for two subjects.

that can identify the components of the model. In contrast to previously used methods, our algorithm does not require hundreds of input-output trials to estimate the state/time-dependent parameters.

Our methodology allowed us to estimate the different parameters of the dynamic ankle stiffness during quasi-stationary and continuous movement experiments. The result presented in Fig. 6 are consistent with previous our knowledge of joint stiffness: when there is activation, the stiffness increases in proportion to the number of engaged cross-bridges [3] and if there are large movements, some of the cross-bridges will be forcibly detached thus reducing the stiffness. When the movement is finalized and if the activation level is maintained, the stiffness should return to its stationary value, as is observed. When there is no activation, there are fewer engaged cross-bridges so this phenomenon is less prominent.

These observations validate our hypothesis that results obtained during stationary experiments cannot be extrapolated to more functional situations.

The modulation of the remainder model parameters will be analyzed in an extended version of this document.

REFERENCES

[1] R. E. Kearney, R. B. Stein, and L. Parameswaran, "Identification of intrinsic and reflex contributions to human ankle stiffness dynamics," *IEEE Trans. on Biomedical Eng*, vol. 44, no. 6, pp. 493 – 504, 1997.

[2] S. K. Au and H. Herr, "Powered ankle-foot prosthesis," *Robotics & automation magazine, IEEE*, vol. 15, no. 3, pp. 52–59, 2008.

[3] E. Burdet, D. W. Franklin, and T. E. Milner, *Human robotics: neuromechanics and motor control*. MIT Press, 2013.

[4] M. M. Mirbagheri, H. Barbeau, and R. E. Kearney, "Intrinsic and reflex contributions to human ankle stiffness: Variation with activation level and position," *Exp Brain Res*, vol. 135, no. 4, pp. 423 – 436, 2000.

[5] J. B. MacNeil, R. E. Kearney, and I. W. Hunter, "Identification of time-varying biological systems from ensemble data (joint dynamics application)," *Biomedical Engineering, IEEE Transactions on*, vol. 39, no. 12, pp. 1213–1225, 1992.

[6] H. Lee and N. Hogan, "Time-varying ankle mechanical impedance during human locomotion," *Neural Systems and Rehabilitation Engineering, IEEE Transactions on*, vol. PP, no. 99, pp. 1–9, 2014.

[7] E. J. Rouse, L. J. Hargrove, E. J. Perreault, and T. A. Kuiken, "Estimation of human ankle impedance during the stance phase of walking," *Neural Systems and Rehabilitation Engineering, IEEE Transactions on*, vol. 22, no. 4, pp. 870–878, July 2014.

[8] D. L. Guarin and R. E. Kearney, "An instrumental variable approach for the identification of time-varying, hammerstein systems,," *Accepted to: 17th IFAC Symposium on System Identification*, 2015.